Desalination and Water Treatment
www.deswater.com
doi: 10.1080/19443994.2014.983178

57 (2016) 1967–1976
January

Taylor & Francis
Taylor & Francis Group

Accumulated impact of operating conditions on the specific cake resistance in dead-end microfiltration mode

Zhan Wang[a], Ximing Zhang[a], Xu Wang[b,*], Yawen Lyu[c]

[a]*Beijing Key Laboratory for Green Catalysis and Separation, Department of Chemistry and Chemical Engineering, Beijing University of Technology, Beijing 100124, P.R. China, Tel. +86 10 6739 6186; emails: wangzhan3401@163.com (Z. Wang), zhangximing@emails.bjut.edu.cn (X. Zhang)*

[b]*Weather Modification Office, Xingjiang Uygur Autonomous Region of China, Urumqi 830002, P.R. China, Tel. +86 0991 2650440; email: wangxu2323@vip.163.com*

[c]*Beijing Rosedale Filter Systems Company, Beijing 100176, P.R. China, Tel. +86 1350 1018802; email: yawen73@163.com*

Received 6 April 2014; Accepted 13 October 2014

ABSTRACT

A series of dead-end unstirred microfiltration experiments were conducted. Impact of different operating conditions (trans-membrane pressure (TMP), temperature, and concentration) on the specific cake resistance (SCR) using yeast suspension and polyethersulfone membranes of 0.1 μm was systematically studied. The results showed that TMP, temperature, and concentration have a significant influence on the SCR. The SCR increased with the increasing concentration and TMP, while decreased with the increasing temperature. The sequence of average accumulated impact of the operating conditions on the SCR was TMP (54.6%) > temperature (−24.2%) > concentration (21.1%). The total accumulated impact of operating conditions on the SCR was 44.5%. This result provides the basis for process optimization and process modeling.

Keywords: Impact; Operating conditions; Specific cake resistance; Dead-end unstirred; Multi-regression method

1. Introduction

As the most commonly sold pressure-driving membrane technology, microfiltration (MF) is widely used in many areas, such as food industry, biotechnology, medicine, drinking water purification, wastewater treatment, the petroleum industry, and the metallurgical industry [1,2]. However, the main obstacle to MF is the flux decline due to the cake formation at the membrane surface and in the pores [3]. Therefore, the characteristics of cake, such as cake thickness, cake porosity, the specific cake resistance (SCR), and cake compressibility play an important role in MF. Among them, the SCR is the most important factor revealed the physical characteristics of the cake [4] and its accurate knowledge is crucial for proper design and scale-up of the practical MF systems [5].

As well-known, the dead-end MF process is more common for large-scale MF applications. In this mode, the SCR is dependent on many factors, such as operating conditions (trans-membrane pressure (TMP), concentration, and temperature) [6,7], particle diameter, particle shape, cake porosity [8], and suspension properties including pH [9–11] and ionic strength [10].

*Corresponding author.

When the suspensions and membrane equipment were specified, as in the real industrial processes, operating conditions (TMP, concentration, and temperature) were the only influencing factors on the SCR. A number of studies are available in the literature that attempt to describe impact of operating conditions on the SCR in MF during dead-end mode: The SCR increases as TMP increased [4,10,12–14], while the SCR dramatically changes with concentration variation [7]. Furthermore, the SCR also changes as the temperature varied [12]. However, up to now, only few quantitative studies about the interactive effects of different operating conditions on the SCR have been found [12]. Moreover, the total accumulated impacts of operating conditions on the SCR for dead-end MF mode have not been well studied yet. So, how to establish the relationship between the SCR and operating conditions, and quantificationally estimate contribution of the different operating conditions to the SCR have a great significance in deeply understanding the filtration process optimization in dead-end MF.

Recognizing importance of the impact of operating conditions on cake formation, this study aims to investigate accumulated effects of the three key operating parameters, such as TMP, concentration, and temperature, on the SCR in dead-end MF mode.

2. Materials

Polyethersulfone (PES) MF membrane with nominal pore sizes of 0.1 μm was used as the filtration medium from Ande Membrane Separation Technology Engineering (Beijing) Co. Ltd. The polytetrafluoroethylene (PTFE) MF membrane with a nominal pore size of 0.2 μm was the second membrane purchased from Beijing Chemical Engineering University Liming Membrane Material Corporation (Beijing, China). Before each experiment, the membranes were soaked in deionized water for 24 h to remove glycerin, which was used as a protectant in the membranes.

Yeast suspension was used in the filtration experiments. Mauri instant dry yeast was produced by Harbin-Mauri Yeast, whose average particle size was 5.1 μm.

$Na_2HPO_4{\cdot}12H_2O$ and KH_2PO_4 were used as the preparation of phosphate-buffered solutions (PBS) obtained from Beijing YILI fine Chemical Engineering, Ltd.

3. The preparation of solution/suspension

3.1. The preparation of phosphate-buffered solution (PBS)

PBS were prepared by dissolving 0.03 M $Na_2HPO_4{\cdot}12H_2O$ and 0.03 M KH_2PO_4 in 1 L deionized and pre-filtered water. Then, the buffer solutions were filtered using a PTFE MF membrane of 0.2 μm at a low pressure (0.01 MPa) to eliminate large or suspended particles.

3.2. The preparation of yeast suspension

Mauri instant dry yeast was dissolved into 800 mL deionized water which was pre-filtered through a 0.2 μm PTFE membrane at 25°C for 30 min with constant stirring. After rehydration, the yeast suspension was centrifuged (LD5-10 model centrifuge, Beijing medical centrifuge factory company) at a speed of 2,500 rpm for 10 min, and then, the supernatant was removed. The above washing process was repeated up to three times. After washing, the yeast was dried at 80°C for 6 h in an oven (WG2003 model Miniature, Chongqing Sida experimental instrument Co. Ltd), and weight of dry yeast was measured. The mass was measured again after 6 h to make sure no weight change had been occurred. Then, a specific amount of this yeast was dissolved into a particular amount of PBS firstly at constant stirring for 20 min and then processed ultrasonically (Ultrasonic generator 235, Academy of science, acoustics graduate school) for 20 min to achieve the desired concentration. In this study, all concentrations of yeast suspensions were referred to the concentrations of the dry washed yeast and the fresh yeast suspensions were prepared daily and generally used within 24 h.

4. Apparatus and method

A dead-end stirred cell with an effective membrane area of $28.0 \times 10^{-4}\,m^2$ was used in the experiments, and the schematic diagram of the system operation is shown in Fig. 1. The MF cell consists of a cylindrical vessel, equipped with a porous support on which the membrane has been placed.

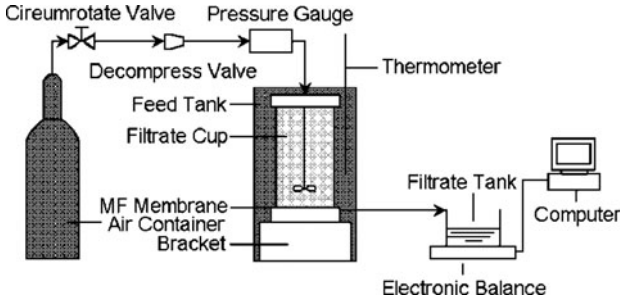

Fig. 1. Schematic diagram of the dead-end MF experimental set-up.

The feed suspensions were introduced into the filtration cell. MF experiments were performed under constant TMP by applying compressed nitrogen gas. The permeate weight was measured during filtration process with an electronic balance (Ohaus Corp Pine Brook. NJ with precision of 0.0001 g). The weights were converted to volumes using density correlations. The temperature of permeate was measured to determine its viscosity and density. The ranges of various operation conditions were chosen at TMP of 0.04–0.12 MPa, concentration of 0.3–2.0 g L^{-1}, and temperature of 20–45 ℃, respectively. The experimental data were recorded after each 30 s.

The MAF-5001 model Malvern laser particle diameter distribution instrument (Britain) was used to get the particle distribution of the feed suspensions, and the modified bubble-point method was used to obtain the pore size distribution of the membrane.

5. Theory and methods

5.1. Fouling mechanism

The blocking law, first proposed by Herman [15], was commonly used to determine the fouling mechanism. In this study, the linear relationship of t/V (filtration time/the total volume of permeate) versus V (the total volume of permeate) was used to determine cake filtration mechanisms.

5.2. Determination of the SCR

Based on cake filtration mechanism, the experimental data from dead-end filtration tests under constant TMP can also be used to evaluate the average SCR ($\bar{\alpha}$) by plotting t/V versus V [16,17].

$$\frac{t}{V} = \frac{R_m \mu}{A_m \Delta P} + \bar{\alpha}\frac{\mu C_0}{2A_m^2 \Delta P} V \tag{1}$$

where t is filtration time (s), V is the total volume of permeate (m^3), A_m is the membrane area (m^2), and C_0 is the concentration of feed of yeast suspension (g L^{-1}).

Eq. (1) showed that the slope of the line was obtained through plotting t/V vs. V, and then, further, it can be used to calculate the average SCR ($\bar{\alpha}$).

5.3. Impact of operating conditions on the SCR

The relationship between the average SCR ($\bar{\alpha}$) and the operating conditions (concentration, temperature, and TMP) was calculated using multiple regressions and expressed by the following formula:

$$\bar{\alpha} = f(C) + \varphi(P) + \omega(T) \tag{2}$$

where C is the concentration of feed suspensions (g L^{-1}),P is TMP (Pa), and T is the temperature (℃).

While the divergence between the experimental data and model-predicted values was quantitatively evaluated in terms of the relative error as expressed by formula (3) as follows:

$$E = 100 \times \frac{|\bar{\alpha}_M - \bar{\alpha}_E|}{\bar{\alpha}_E} \tag{3}$$

where $\bar{\alpha}_M$ is model-predicted average SCR (m kg^{-1}) and $\bar{\alpha}_E$ is experimental average SCR (m kg^{-1}).

Impact of operating conditions on the average SCR ($\bar{\alpha}$) can be defined by the following formula (4):

$$I_x = \frac{\partial \bar{\alpha}}{\partial x} = \psi'(x) \tag{4}$$

where x is operating condition, such as TMP, concentration, and temperature, respectively.

5.4. The accumulated impact of operating conditions on the SCR

The accumulated impact of each operating condition x (A_x) on the average SCR ($\bar{\alpha}$) in the range of $x_1 \le x \le x_2$ can be expressed by formula (5) as follows:

$$A_x = \int_{x_1}^{x_2} I_x dx = \int_{x_1}^{x_2} \psi'(x)dx = \psi(x_2) - \psi(x_1) \tag{5}$$

where A_x reflects the accumulated impact of each operating condition x on the average SCR ($\bar{\alpha}$) in the range of $x_1 \le x \le x_2$.

The total accumulated impact of different operating conditions (C, TMP, and T) on the average SCR ($\bar{\alpha}$) in the range of $C_1 \le C \le C_2$, $TMP_1 \le TMP \le TMP_2$, and $T_1 \le T \le T_2$ can be expressed using formula (6) as follows:

$$A = A_C + A_P + A_T = \int_{C_1}^{C_2} I_C dC + \int_{P_1}^{P_2} I_P dP + \int_{T_1}^{T_2} I_T dT \tag{6}$$

where A reflects the total accumulated impact of different operating conditions (C, TMP, and T) on the average SCR ($\bar{\alpha}$) in the range of $C_1 \le C \le C_2$, $TMP_1 \le TMP \le TMP_2$, and $T_1 \le T \le T_2$.

If $A > 0$, it means that the total accumulated impact of these operating conditions on the average SCR ($\bar{\alpha}$) in the joint space is positive, and the average SCR ($\bar{\alpha}$) increased with increasing concentration, temperature, and TMP. In contrast, $A < 0$ means that total accumulated impact of these operating conditions on the average SCR ($\bar{\alpha}$) in joint space is negative, and the average SCR ($\bar{\alpha}$) decreases with increasing concentration, temperature, and TMP.

5.5. The average contribution of different operating conditions on the average SCR

The average contribution of the different operating conditions (concentration, temperature, and TMP) on the average SCR ($\bar{\alpha}$) can be expressed by the following formula (7):

$$P\% = \frac{A_i}{\sum A_i} = \frac{A_i}{|A_P| + |A_T| + |A_C|} \times 100\% \quad (7)$$

where i represents concentration, temperature, and trans-membrane pressure, respectively.

5.6. Determination of compressibility of the yeast cakes

For most compressible cakes, the relation between the specific resistance of the cake and ΔP is represented by formula (8) as follows:

$$\alpha = \alpha_0 \Delta P^n \quad (8)$$

where α is the SCR, α_0 is a constant, and n is the compressibility of the cake which can be calculated from the slope of line between ln α and ln ΔP. Using above Eq. (8), the compressibility exponent, n, was determined to be 0.36 for yeast suspensions in the present dead-end MF. Hence, the yeast cake was compressible.

6. Results and discussion

6.1. The filtration characteristics

The filtration capacity of the membrane was revealed useful information of the mechanism and the status of the membrane fouling. A series of the experiments were conducted under different operating conditions (concentration, TMP, and temperature) using yeast suspensions with PES membrane of 0.1 μm. One arbitrary result of them is shown in Fig. 2.

It can be seen from Fig. 2(a), the membrane flux decays gradually with time due to membrane fouling [17]. Because the mean size of the yeast particles (5.1 μm) (Fig. 3(a)) is much larger than the nominal membrane pore size of the PES membrane (0.1 μm) Fig. 3(b), so the particles cannot enter the pores but can be responsible for the cake formation at the membrane surface. This is also approved by a linear relationship of t/V versus V as shown in Fig. 2(b), after the first few seconds, the cake filtration model could be applied up to the end of the run. Nearly, all experimental data could be described by the cake filtration model. However, cake filtration is the predominant mechanism in this situation, and this is also found in good agreement with that result, presented in our previous report [18].

6.2. Effect of operating conditions on the average SCR

In order to determine the contribution of the different operating conditions to the average SCR ($\bar{\alpha}$), it is

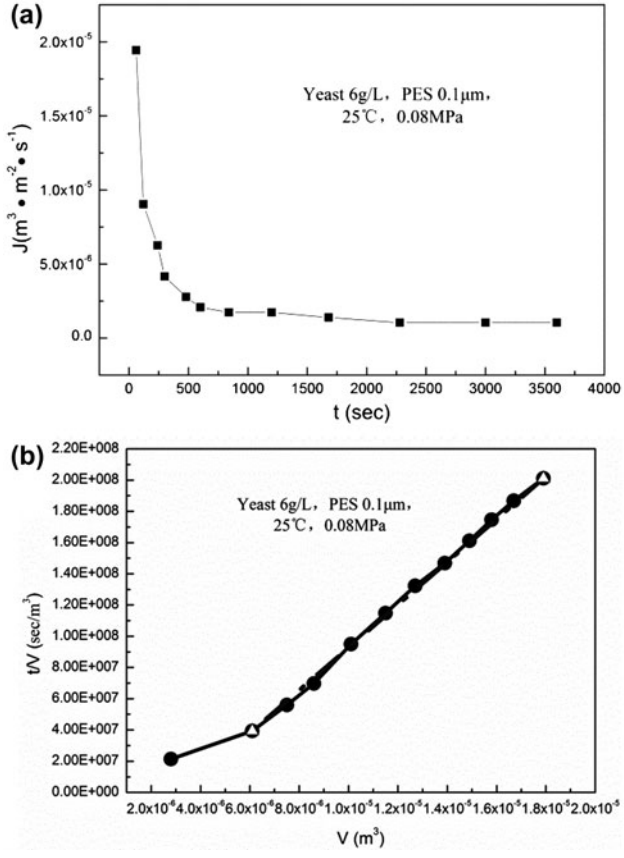

Fig. 2. The filtration characteristics of the PES membrane and determination of the membrane fouling mechanism. Experimental condition: yeast 6 g L^{-1}, PES 0.1 μm, 25℃, 0.08 MPa. (a) The fluxes of the membrane with time for PES membrane of 0.1 μm. (b) Determinationof the cake formation mechanism.

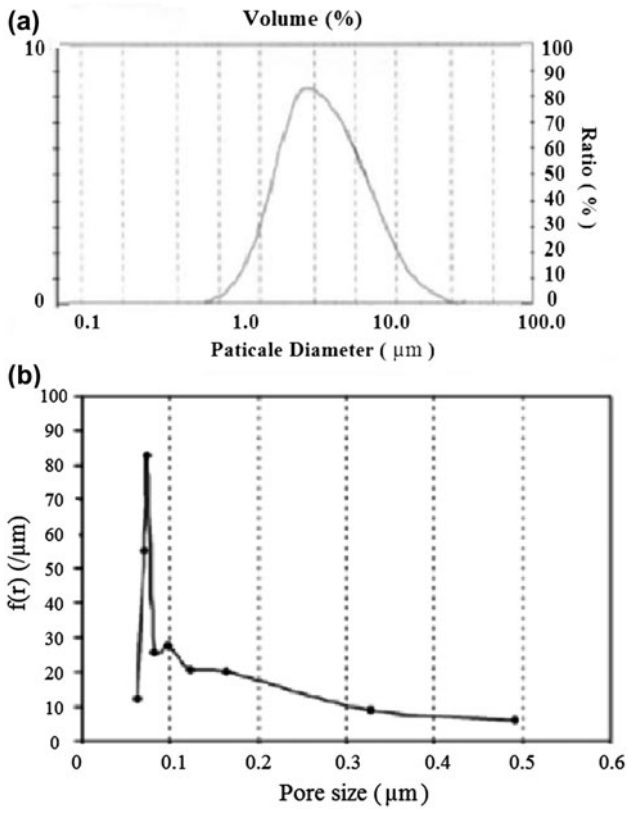

Fig. 3. Particle diameter distribution of yeast suspension (a) and pore size distribution of PES membrane (b).

important to establish the multiple regressions to model the experimental data. A series of the experiments of yeast suspension using PES of 0.1 μm were carried out and five different equations, such as linear equation, logarithmic equation, polynomial, power function, and exponential function, were used to fit experimental data, respectively, and the results were shown in Table 1.

By comparing the correlation coefficient of determination (R^2) and significance level (p) of multiple regressions in Table 1, the most suitable mathematical expressions were selected for different conditions, respectively, and were used to predict experimental data as shown in Fig. 4.

As presented in Fig. 4(a), $\bar{\alpha}_C$ initially increases to a maximum with respect to concentration before falling back to a lower value. This can be explained by the reason that before the concentration reaches a certain value, the cake porosity would decline due to the less solute particles preferentially entering into cake [19], which would leads to increase $\bar{\alpha}_C$. When the concentration exceeds a certain value, the increase in both bridge of particles and cake porosity caused the reduction in $\bar{\alpha}_C$. The most suitable second-order univariate polynomial agreed well with the experimental data, and it can be expressed by the formula (9) as follows:

$$\bar{\alpha}_C = -2.121 \times 10^{14} C^2 + 5.683 \times 10^{14} C + 1.404 \times 10^{14} (R^2 = 0.8807, p = 0.119) \quad (9)$$

It can be seen from Fig. 4(b), $\bar{\alpha}_P$ increases sharply with increasing TMP. The reason is that, although rising TMP can elevate and increase the permeate flux, it also enhance the convective flow of particle toward the membrane surface, which subsequently enhances the deposition of particle at membrane surface and in pores. Moreover, the rising TMP can also accelerate the growing rate of cake deposition and result in the cake compactness due to the rearrangement and transmutation of solid particles [20] or the fracture of coacervate. The most suitable second-order univariate polynomial agreed well with the experimental data, and it can be expressed by the formula (10) as follows:

$$\bar{\alpha}_p = 5.136 \times 10^{16} P^2 - 3.797 \times 10^{15} P + 3.548 \times 10^{14} (R^2 = 0.8905, p = 0.109) \quad (10)$$

As shown in Fig. 4(c), in most cases, $\bar{\alpha}_T$ decreases with increasing temperature . The reason is explained as follows: As temperature increases, the higher permeate flux will be obtained at higher temperature due to lower value of the viscosity and higher mass-transfer coefficient according to the film model [20,21]. Moreover, these facts make the drag force for solute particles to increase and the bridge phenomena become insignificant. As a result, solute particles deposit uneasily on the membrane surface and the formed cake will be lost. So therefore, temperature is inversely proportional to the $\bar{\alpha}_T$ in most cases. However, extremes of temperature can also make cake harder [22] and cause the increase in $\bar{\alpha}_T$. The most suitable second-order univariate polynomial again agreed well with the experimental data, and it can be expressed by the formula (11) given as follows:

$$\bar{\alpha}_T = 4.813 \times 10^{11} T^2 - 3.755 \times 10^{13} T + 1.087 \times 10^{15} (R^2 = 0.9558, p = 0.044) \quad (11)$$

6.3. Quantitative analysis of total accumulated effect of operating conditions on the average SCR

The previous studies showed that the average SCR ($\bar{\alpha}$) changed nonlinearly with the operating conditions (concentration, TMP, and temperature) as

Table 1
The choice of the most suitable multiple regressions

Operating condition	Equation	R^2	F	p
C = 0.3–2.0 g L^{-1}, TMP = 0.12 MPa, T = 25 ℃	$Y = 8.622 \times 10^{13}X + 3.294 \times 10^{14}$	0.3813	1.849	0.267
	$Y = 9.844 \times 10^{13}\mathrm{Ln}(X) + 4.365 \times 10^{14}$	0.6170	4.833	0.115
	$Y = -2.121 \times 10^{14}X^2 + 5.683 \times 10^{14}X + 1.404 \times 0^{14}$	0.8807	7.382	0.119
	$Y = 4.281 \times 10^{14}X^{0.2731}$	0.6297	5.102	0.109
	$Y = 3.172 \times 10^{14}e^{0.2418X}$	0.3977	1.981	0.254
TMP = 0.04–0.12 MPa, C = 2.0 g L^{-1}, T = 25 ℃	$Y = 4.420 \times 10^{15}X + 6.720 \times 10^{13}$	0.8279	14.432	0.016
	$Y = 3.071 \times 10^{14}\mathrm{Ln}(X) + 1.218 \times 10^{15}$	0.7521	9.102	0.057
	$Y = 5.136 \times 10^{16}X^2 - 3.797 \times 10^{15}X + 3.548 \times 10^{14}$	0.8905	8.132	0.109
	$Y = 2.706 \times 10^{15}X^{0.7358}$	0.8564	17.891	0.024
	$Y = 1.759 \times 10^{14}e^{10.29X}$	0.8900	24.273	0.032
T = 20–45 ℃, TMP = 0.04–0.12 MPa, C = 0.3–2.0 g L^{-1}	$Y = -6.070 \times 10^{12}X + 6.090 \times 10^{14}$	0.6878	6.609	0.082
	$Y = -2.020 \times 10^{14}\mathrm{Ln}(X) + 1.107 \times 10^{15}$	0.7936	11.535	0.043
	$Y = 4.813 \times 10^{11}X^2 - 3.755 \times 10^{13}X + 1.087 \times 10^{15}$	0.9558	21.624	0.044
	$Y = 1.970 \times 10^{15}X^{-0.4576}$	0.8240	14.045	0.033
	$Y = 6.395 \times 10^{14}e^{-0.01383X}$	0.7224	7.807	0.068

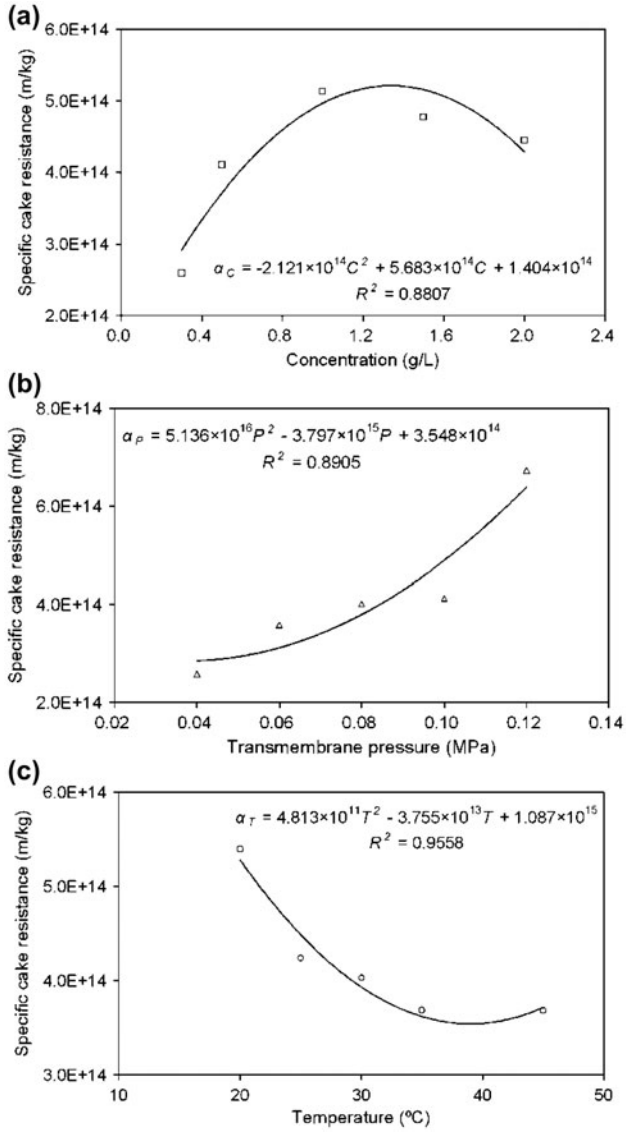

Fig. 4. Validation of the most suitable mathematical expressions with yeast suspension under different concentration (*C*), TMP and the temperature (*T*). (a) The average SCR ($\bar{\alpha}$) as function of feed concentration (C). (b) The average SCR ($\bar{\alpha}$) as function of the TMP. (c) The average SCR ($\bar{\alpha}$) as function of the temperature (T).

the second-order univariate polynomial. So, in order to provide the basis to optimize the membrane filtration process, we will express the total accumulated influence of operating conditions on the average SCR ($\bar{\alpha}$) by the second-order univariate polynomial as given in the following formula (12):

$$\bar{\alpha} = a_1C^2 + a_2C + b_1P^2 + b_2P + c_1T^2 + c_2T + d \quad (12)$$

After multiple regressions, the following total accumulated equation between average SCR ($\bar{\alpha}$) and operating conditions ($R^2 = 0.7907$, $p = 0.004$) can be expressed by formula (13) as follows:

$$\bar{\alpha} = 7.403 \times 10^{14} - 2.121 \times 10^{14}C^2 + 5.683 \times 10^{14}C + 5.136 \times 10^{16}P^2 - 3.797 \times 10^{15}P + 4.813 \times 10^{11}T^2 - 3.755 \times 10^{13}T \quad (13)$$

The relative error between the predicted values by Eq. (13) and calculated values by Eq. (1) is shown in Table 2. It can be seen from Table 2, the relative errors lie in the range from 4.8% to 16.6%, and the average absolute error is less than 10%. This result demonstrates the reliability of the Eq. (13).

As illustrated in Fig. 5, the influencing degree of single concentration (*C*), TMP (*P*), and temperature (*T*) on the average SCR ($\bar{\alpha}$) can be expressed as follows: $I_C = -4.242 \times 10^{14}C + 5.683 \times 10^{14}$, $I_P = 1.027 \times 10^{17}P - 3.797 \times 10^{15}$, and $I_T = 9.626 \times 10^{11}T - 3.755 \times 10^{13}$, respectively.

It can be seen from Fig. 5, I_C decreases from 4.41×10^{14} to -2.80×10^{14} g/L with increasing concentration from 0.3 to 2.0 g L^{-1}. The variation extent of I_C was7.21×10^{14} g/L. The contribution of concentration to the average SCR ($\bar{\alpha}$) is positive firstly, and then, it became negative. In other words, $\bar{\alpha}$ increases with increased concentration until 1.3 g L^{-1}, but this trend became weaker and weaker gradually. In contrast, the average SCR ($\bar{\alpha}$) decreases with increasing concentration, when concentration is higher than 1.3 g L^{-1}, then, this trend becomes more strong. Similarly, I_P increases from 0.31×10^{15} to 8.53×10^{15} MPa with increasing TMP from 0.04 to 0.12 MPa, and the variation extent of I_P is 8.22×10^{15} MPa, the contribution of TMP to the average SCR ($\bar{\alpha}$) is positive and the average SCR ($\bar{\alpha}$) increases with increasing TMP. Whereas I_T changes from -1.83×10^{13} to 0.58×10^{13} °C with increasing temperature from 20 to 45°C, the variation extent of I_T is 2.41×10^{13} °C. The contribution of the temperature to the average SCR ($\bar{\alpha}$) is negative firstly, and then, it became positive. In other words, the average SCR ($\bar{\alpha}$) decreases with increasing temperature until 39°C, but this trend became weaker and weaker gradually. In contrast, the average SCR ($\bar{\alpha}$) increases with increased temperature when temperature is greater than 39°C, and this trend became stronger.

Table 2
The relative error calculated by Eq. (3) using the predicted values by Eq. (13) and corresponding calculated values by Eq. (1)

C (g L^{-1})	P (MPa)	T (℃)	$\bar{\alpha}$ (by Eq. (13)) (10^{14} m kg^{-1})	$\bar{\alpha}$ (by Eq. (1)) (10^{14} m kg^{-1})	E (%)	Average (%)
0.4	0.05	20	3.14	2.88	8.2	9.8
1	0.08	25	4.84	4.15	16.6	
2	0.10	45	4.47	4.95	9.7	
1.6	0.11	30	6.17	5.89	4.8	

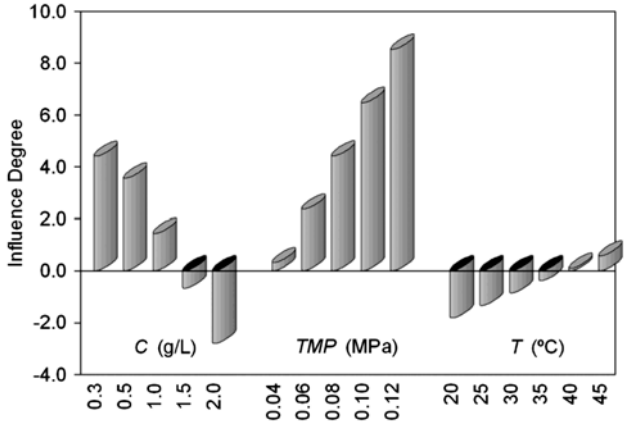

Fig. 5. Influencing degree of different operating conditions on the average SCR ($\bar{\alpha}$) in dead-end unstirred mode. Influencing degree of feed concentration I_C (10^{14} mL kg^{-1} g), of TMP I_P (10^{14} m L kg^{-1} g) and of temperature I_T (10^{12} m kg^{-1} ℃).

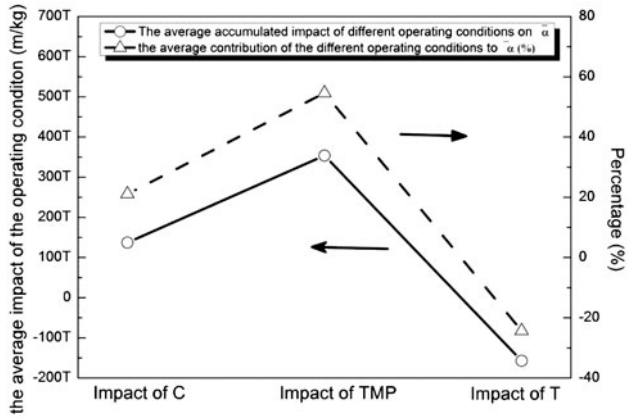

Fig. 6. The average accumulated impact of different operating conditions on the average SCR ($\bar{\alpha}$) and the average contribution of the different operating conditions to the average SCR ($\bar{\alpha}$).

6.4. The average accumulated impact of the operating conditions on the average SCR

In the concentration range 0.3–2.0 g L^{-1}, the accumulated impact of concentration (A_C) on the average SCR ($\bar{\alpha}$) is 1.37×10^{14} m kg^{-1}, this means that the contribution of C to the average SCR ($\bar{\alpha}$) is positive. Similarly, in TMP range 0.04–0.12 MPa, $A_P = 3.54 \times 10^{14}$ m kg^{-1}, the contribution of TMP to the average SCR ($\bar{\alpha}$) is positive. In the temperature range 20–45℃, $A_T = -1.57 \times 10^{14}$ m kg^{-1}, the contribution of T to the average SCR ($\bar{\alpha}$) is negative. The absolute rations of A_P, A_T, and A_C are 2.6: 1.1.1, and the average contributions of the concentration, temperature, and TMP to the average SCR are 21.1, −24.2, and 54.6%, respectively, as shown in Fig. 6. Therefore, the sequence of average accumulated impact of different operating conditions on the average SCR ($\bar{\alpha}$) is $A_P > A_T > A_C$.

If considering operating conditions in joint space 0.3–2.0 g L^{-1}, 0.04–0.12 MPa, and 20–45℃, the average total accumulated impact of operating conditions on the average SCR ($\bar{\alpha}$) was found 3.34×10^{14} m kg^{-1}, this means that the average SCR ($\bar{\alpha}$) increases with increased concentration, temperature, and TMP. Furthermore, $\frac{A}{\bar{\alpha}_{MAX}-\bar{\alpha}_{MIN}} = \frac{A_P+A_T+A_C}{\bar{\alpha}_{MAX}-\bar{\alpha}_{MIN}} = \frac{3.34\times10^{14}}{8.4099\times10^{14}-0.8960\times10^{14}} = 44.5\%$, this means that the average impact of operating conditions on average SCR ($\bar{\alpha}$) is 44.5%, or we can say that the average SCR ($\bar{\alpha}$) could be changed 44.5% by changing these operating conditions.

Conclusion

The effect of total accumulated interactions of various operating conditions on the average SCR ($\bar{\alpha}$) in dead-end unstirred MF cell at different operating conditions (concentration, TMP, and temperature) using PES of 0.1 μm was analyzed. The following results were obtained:

(1) Concentration (C), TMP (P), and temperature (T) were all the influential factors for the average SCR ($\bar{\alpha}$), and $\bar{\alpha}$ was changed with these operating conditions as $\bar{\alpha} = 7.403 \times 10^{14}-$

$2.121 \times 10^{14}C^2 + 5.683 \times 10^{14}C + 5.136 \times 10^{16}P^2 - 3.797 \times 10^{15}P + 4.813 \times 10^{11}T^2 - 3.755 \times 10^{13}T$.

(2) Both contributions of concentration and TMP to the average SCR ($\bar{\alpha}$) were found positive. In contrast, the contribution of temperature to the average SCR ($\bar{\alpha}$) was negative. The sequence of impact of the operating conditions on the average SCR ($\bar{\alpha}$) was obtained in the order as TMP (54.6%) > temperature (−24.2%) > concentration (21.1%). Therefore, the average total accumulated impact of operating conditions on the average SCR ($\bar{\alpha}$) in joint space of the operating conditions was 44.5%. This means that the operating conditions could be used to control the average SCR ($\bar{\alpha}$) and it can be used to provide the basis to process optimization and modeling for membrane rinsing process.

Acknowledgments

We thank Ms Hamida Panezai for editorial assistance. Support for this work was provided by National Natural Science Foundation of China (Project NO. 21176006, 21476006 and NO. 21387009 (212111078)).

Nomenclature

A — the total accumulated impact of operating conditions on the average SCR (m kg^{-1})
A_m — the effective area of the membrane (m^2)
A_x — the accumulated impact of each operating condition x on the average SCR (m kg^{-1})
C — feed concentration (g L^{-1})
C_0 — feed concentration (g L^{-1})
E — relative error (%)
F — test statistic
I — the impact of operating condition on the SCR
J — membrane permeate flux (m s^{-1})
J_0 — the pure water flux of the membrane (m s^{-1})
Δp — TMP drop (MPa)
p — significance level
T — temperature (°C)
t — filtration time (s)
R^2 — the coefficient of determination
R_m — intrinsic membrane resistance (m^{-1})
x — operating conditions
V — the accumulated permeate volume (m^3)

Greeks

$\bar{\alpha}$ — the average SCR (m kg^{-1})
$\bar{\alpha}_C$ — average SCR as function of feed concentration (m kg^{-1})
$\bar{\alpha}_E$ — experimental average SCR (m kg^{-1})
$\bar{\alpha}_M$ — model predicted average SCR (m kg^{-1})
$\bar{\alpha}_P$ — average SCR as function of TMP drop (m kg^{-1})
$\bar{\alpha}_T$ — average SCR as function of temperature (m kg^{-1})
f — function of feed concentration
ϕ — function of TMP drop
ω — function of temperature
ψ — function of operating conditions
μ — permeate viscosity (Pa s)

References

[1] J. Shi, Q. Yuan, C.J. Gao, Membrane Technology Handbook, Chemistry Industry Press, Bejing, 1998.
[2] Y.H. Gao, L.B. Ye, Foundation of Membrane Separation Technology, Science Press, Beijing, 1989.
[3] B. Tansel, W.Y. Bao, I.N. Tansel, Characterization of fouling kinetics in ultrafiltration systems by resistances in series model, Desalination 129 (2000) 7–14.
[4] J. Cho, K.G. Song, K.H. Ahn, The activated sludge and microbial substances influences on membrane fouling in submerged membrane bioreactor: Unstirred batch cell test, Desalination 183 (2005) 425–429.
[5] S.K. Teoh, Reginald B.H. Tan, C.T. Tien, A new procedure for determining specific filter cake resistance from filtration data, Chem. Eng. Sci. 61 (2006) 4957–4965.
[6] E. Iritani, Y. Mukai, Y. Tanaka, T. Murase, Flux decline behavior in dead-end microfiltration of protein solutions, J. Membr. Sci. 103 (1995) 181–191.
[7] J. Sripui, C. Pradistsuwana, W.L. Kerr, P. Pradipasena, Effects of particle size and its distribution on specific cake resistance during rice wine microfiltration, J. Food. Eng. 105 (2011) 73–78.
[8] S.A. Lee, A.G. Fane, R. Amal, The effect of floc size and structure on specific cake resistance and compressibility in dead-end microfiltration, Sep. Sci. Technol. 38 (2003) 869–887.
[9] N.M. Jenny, G. Foley, Dead-end filtration of yeast suspensions: Correlating specific resistance and flux data using artificial neural networks, J. Membr. Sci. 281 (2006) 325–333.
[10] K. Ohmori, C.E. Glatz, Effects of pH and ionic strength on microfiltration of *C. glutamicum*, J. Membr. Sci. 153 (1999) 23–32.
[11] M. Mota, J.A. Teixeira, Influence of cell-shape on the cake resistance in dead-end and cross-flow filtrations, Sep. Purif. Technol. 27 (2002) 137–144.
[12] X. Ye, J. Yao, Z. Wang, D. Liu, Application of linear multi-regression model for specific resistance study in the dead-end microfiltration, J. Beijing University Technol. 11 (2007) 211–216.
[13] J. Lee, W.Y. Ahn, C.H. Lee, Comparison of the filtration characteristics between attached and suspended growth microorganisms in submerged membrane bioreactor, Water Res. 35 (2001) 2435–2445.
[14] S.K. Zaidi, A. Kumar, Experimental analysis of a gel layer in dead-end ultrafiltration of a silica suspension, Desalination 172 (2005) 107–117.
[15] J. Hermia, Trans. IChemE. 60 (1982) 183–187.
[16] D.C. Sioutopoulos, A.J. Karabelas, S.G. Yiantsios, Organic fouling of RO membranes: Investigating the correlation of RO and UF fouling resistances for predictive purposes, Desalination 261 (2010) 272–283.

[17] M. Pontié, A. Thekkedath, K. Kecili, H. Dach, F. De Nardi, J.B. Castaing, Clay filter-aid in ultrafiltration (UF) of humic acid solution, Desalination 292 (2012) 73–86.
[18] Z. Wang, J. Chu, X. Zhang, Study of a cake model during stirred dead-end microfiltration, Desalination 217 (2007) 127–138.
[19] G. Foley, P.F. MacLoughlin, D.M. Malone, Preferential deposition of smaller cells during cross-flow microfiltration of a yeast suspension, Biotechnol. Tech. 6 (1992) 115–120.
[20] T.B. Choe, P. Masse, A. Verdier, Membrane fouling in the ultrafiltration of polyelectrolyte solutions: Polyacrylic acid and bovine serum albumin, J. Membr. Sci. 26 (1986) 17–30.
[21] F.B. Javier, A.L. Juan, A.I. Leal, M. González, The use of ultrafiltration and nanofiltration membranes for the purification of cork processing wastewater, J. Hazard. Mater. 162 (2009) 1438–1445.
[22] M. Bartlett, M.R. Bird, J.A. Howell, An experimental study for the development of a qualitative membrane cleaning model, J. Membr. Sci. 105 (1995) 147–157.